Disponible en ligne sur www.sciencedirect.com
ScienceDirect
C. R. Chimie 13 (2010) 212–226
Comptes Rendus Chimie

Account / Revue

Thin film photochromic materials: Effect of the sol-gel ormosil matrix on the photochromic properties of naphthopyrans

Rosario Pardo, Marcos Zayat, David Levy *

Instituto de Ciencia de Materiales de Madrid, C.S.I.C., 28049 Cantoblanco, Madrid, Spain

Received 30 March 2009; accepted after revision 27 May 2009
Available online 3 July 2009

Abstract

Photochromic naphthopyran derivatives have been embedded in sol-gel prepared organically modified thin films. The introduction of organic functional groups into a silica matrix allows tailoring the surface of its pores and the polarity of the environment of the embedded host molecules. The photochromic properties of the naphthopyran molecules, such as the spectral properties of the coloured forms and the kinetics of the thermal bleaching, depend strongly on the polarity of the pores where the molecules are located and, hence, on the nature and loading of organic functional groups in the composition of the ormosil matrix. Important changes in the photochromic properties of the films have also been induced by modifications in the sol-gel preparation and processing parameters. The photostability of the photochromic molecules upon prolonged exposition to UV light is strongly related to the nature of the embedding ormosil matrix. The introduction of organic functional groups into the inner pore surface of the matrix, where the dye molecules will be located, affects the stability of the molecules, in terms of the effectiveness of the interaction between the photochromic molecules and the pore surface. ***To cite this article: R. Pardo et al., C. R. Chimie 13 (2010).***

Keywords: Photochromism; Naphthopyrans; Sol-gel process; Ormosil; Photostability; Thin films

1. Introduction

Naphthopyrans compounds are known to exhibit photochromism since the first report of Becker and Michl in the early 1960's [1]. The photochromism of these molecules involves a photo-induced cleavage of the C(sp^3)—O bond of the pyran ring, leading to the formation of coloured merocyanine structures. The system reverts thermally to its original colourless form [2], as shown in Fig. 1. Photochromic naphthopyrans can be divided into two groups the 3H-naphtho[2,1-b]pyran (3H-NP) and the 2H-phtho[1,2-b]pyran (2H-NP), being the coloured forms of the molecules from the 2H-NP group more stable than the corresponding 3H-NP molecule, due to the strong steric interaction between the hydrogen atoms in the open quinoidal form of the 3H-NP (Fig. 1) affecting its stability [2].

Naphthopyran derivatives have been studied extensively owing to the possibility of obtaining a photochromic response in a wide range of the visible spectrum from yellow to red [3–5]. The industrial interest of these materials started in the early 1990's, and was directed to the preparation of photochromic ophthalmic lenses [6,7]. Nowadays, these photochromic compounds are also used in architecture, automotive industry, cosmetics, textiles, decoration, etc [8–12]. Most of the scientific research done on photochromic

* Corresponding author.
E-mail addresses: rpardo@icmm.csic.es (R. Pardo), Marcos.-Zayat@icmm.csic.es (M. Zayat), d.levy@icmm.csic.es (D. Levy).

1631-0748/$ – see front matter
doi:10.1016/j.crci.2009.05.006

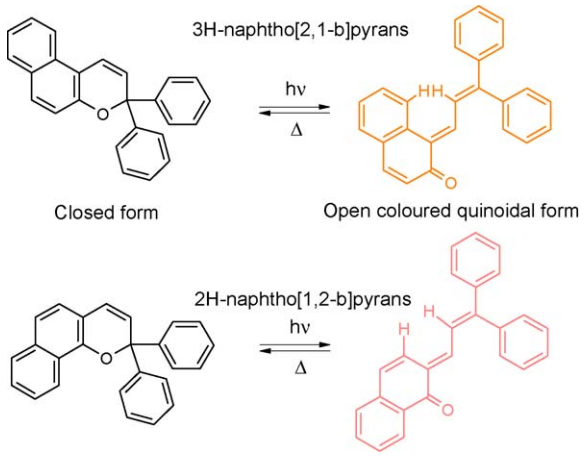

Fig. 1. Bleached and coloured forms of photochromic naphthopyrans.

NP compounds was devoted to the optimization of its spectral and kinetic properties by substitution of functional groups in the photochromic molecule [13–21]. The most remarked properties of these materials, such as the absorption spectra upon irradiation with UV light and the kinetic of the bleaching process (recovery of original whiteness) have been measured in different solvents [4,22–24] or dispersed in organic polymer matrices [7,21,25]. The usage of polymer matrices is a good choice for the entrapment of photochromic molecules; however, it is limited by the low stability of the matrix upon UV irradiation [26,27]. The sol-gel method is a very useful tool to prepare porous inorganic matrices at low temperature [28], to which organic materials can be incorporated. The incorporation of photochromic molecules into sol-gel glasses was firstly reported in the late 1980's [29,30], consisting of molecules of the spiropyran family embedded in organically modified silica glasses. The intense research work done on this field was mainly devoted to dispersions of molecules of the spiropyran and spirooxazine families in sol-gel matrices [31–34]. Samples were also prepared as thin coatings on glass substrates [35–39]. We have recently demonstrated the feasibility of introducing photochromic naphthopyran derivatives into sol-gel ormosil matrices [40] and the effect of different organic functional substituents in the matrix on the photochromic properties of the embedded molecules [41–43].

The photochromic films can find application as variable optical transmission materials, waveguide/fiber-optics optical delay generators [44,45], optical memory devices [46], holographic recording media [47], non-linear optics [48], UV sensors, etc.

2. Ormosil matrices used for the preparation of the photochromic coatings

The preparation of photochromic coatings, via the incorporation of photoactive molecules in vitreous matrices by the sol-gel method, requires the formulation of an initial sol that allows obtaining vitreous transparent films with good optical properties. The introduction of photochromic dyes into this sol is limited by the low stability of the dyes in the acidic medium of acid catalyzed sols. In this sense, acetoxy precursors were chosen, which release acetic acid slowly during hydrolysis, leading to a gentle catalysis of the sol [40].

Several matrices and compositions were studied to allow the incorporation of large amounts of photochromic dye while maintaining a low organic content in the matrix structure. These matrices were prepared from mixtures of silicon alkoxides, [as the tetraacetoxysilane, TAS—$Si(OCOCH3)_4$], with silicon alkoxides modified with organic groups (RTES). These organic groups [$R = -CH_3$ (Me), $-C_2H_5$ (Et), $-C_3H_7$ (Pr), $-C_4H_9$ (iBu), $-C_6H_5$ (Ph) and $-C_6F_5$ (pFPh)] incorporated in the matrix network affect the chemical composition of the inner pore surface (organic functional groups/OH groups ratio), and are, therefore, responsible for the properties of the pore environment where the photochromic molecules are located (Fig. 2). The *R* groups used for the preparation of the different matrices were selected from size and polarity considerations and interaction/affinity with the photochromic dye. Fig. 2 shows a scheme of the pore surface in unmodified and *R*-modified matrix where the dye molecules are located.

The thickness of the films can be controlled using the ormosil matrix via the incorporation of different organic groups or different amounts of these groups, as shown in Fig. 3. An increase of the size or amount of the *R* groups in the matrix results in an increase of the thickness of the films, as shown in Fig. 3a and b, respectively.

The ormosil coatings allow the incorporation of a large amount of photochromic dye and the control of the thickness as well as the inner structure of the matrix where the dye molecules are located. The ability to control these parameters allows controlling the coloration and properties of the photochromic film, which will be of a great interest from the point of view of future applications.

2.1. Preparation of coatings

Samples were prepared from mixtures of tetraacetoxysilane (TAS) and organically modified triethox-

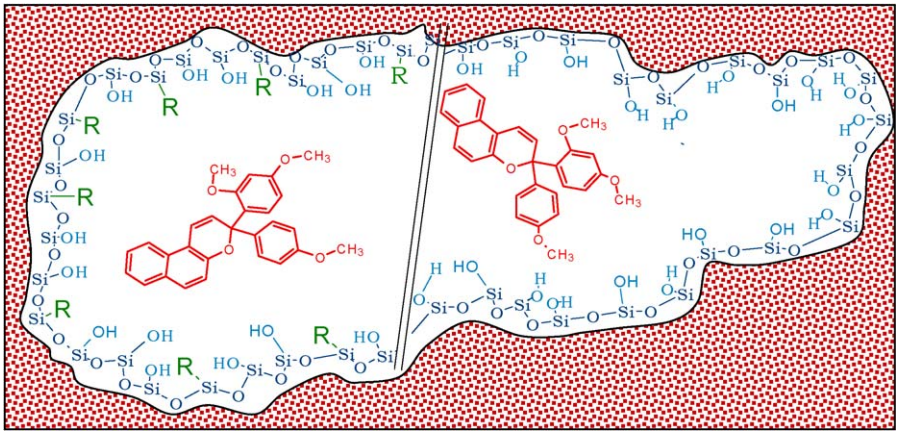

Fig. 2. Scheme of the pore in unmodified (left) and *R* functionalized matrix (right) where the photochromic molecules are located.

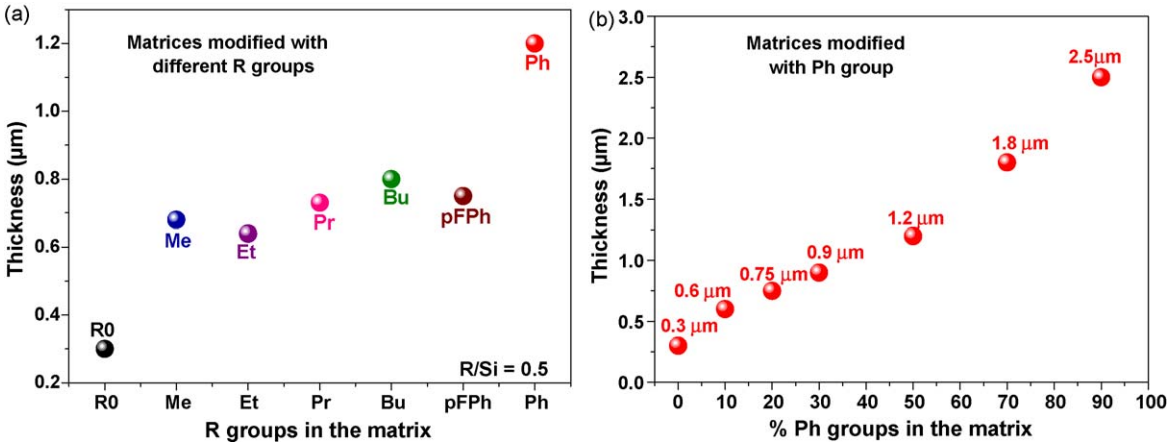

Fig. 3. Thickness of the films prepared with different *R* groups (a) and different amount of Ph group (b).

ysilanes (RTES), where *R* is the organic functional substituent in the ormosil precursor (Me, Et, Pr, iBu, Ph, and pFPh), in the appropriate ratio (Table 1). The ratio of water to hydrolyzing group was kept 1:1 in all samples. The reaction was self-catalyzed by the slow release of acetic acid from the TAS during hydrolysis. The sols were allowed to hydrolyze for 24 h under stirring at 25 °C. The photochromic dye was added as a THF solution, after the hydrolysis of the sol, to obtain the required photochromic-dye/Si molar ratios. THF was used as solvent due to its good miscibility with the coating sol. Fig. 4 shows a representative scheme of the preparation process of the coatings.

The deposition of the films on glass slides was carried out after the addition of the dye using the spin-coating technique (Fig. 4). A sol volume of 0.1 mL was used for the preparation of each film with the sample-holder spinning at 2000 rpm. The films were cured for 24 h at 100 °C.

2.2. Characterization of the samples

The photochromic samples were irradiated with a 365 nm, 100 W, B-100AP UV lamp from UVP, giving a UV-light intensity on the sample of 8.9 mW/cm^2. The absorption spectra of the resulting films as well as the kinetics of the bleaching at dark were measured in a Varian Cary 50 Bio UV–visible spectrophotometer. The absorption spectra were measured between 300 and 800 nm, and are given as ΔAbs ($A_{a.i.}-A_{b.i.}$), where $A_{a.i.}$ and $A_{b.i.}$ are the absorption after and before irradiation, respectively. The bleaching of the photochromic effect was monitored versus time at the wavelength of the maximum absorption of each sample (visible) at 25 °C. The kinetic constants were calculated from the bleaching curves using a bi-exponential decay equation. $t_{1/2}$ is defined as the time required by the sample to reach $\Delta Abs_{max}/2$ during the thermal bleaching. The thickness of the films was

Table 1
Chemical composition of the sols used for film deposition.

Sample name	Molar composition			
	TAS	RTES	H_2O	*R*/Si
R90	0.20	1.80	6.20	0.90
R70	0.60	1.40	6.60	0.70
R50	1.00	1.00	7.00	0.50
R30	1.40	0.60	7.40	0.30
R20	1.60	0.40	7.60	0.20
R10	1.80	0.20	7.80	0.10
R8	1.84	0.16	7.84	0.08
R6	1.88	0.12	7.88	0.06
R4	1.92	0.08	7.92	0.04
R2	1.96	0.04	7.96	0.02
R0	2.00	0	8.00	0

R accounts for Me, Et, Pr, iBu, pFPh and Ph.

measured with a surface roughness measuring system Surftest SV-3000H4.

3. Photochromic naphthopyrans embedded in sol-gel prepared ormosil coatings

Different photochromic naphthopyran derivatives have been incorporated in a sol-gel prepared ormosil matrix and characterized their photochromic properties. In order to have a significant colour change in a thin film of about 1 µm, very high concentrations of the photochromic dye are required. Fig. 5 shows the chemical structure of the different photochromic dyes.

The resulting coatings are transparent, colourless and show a rapid coloration upon exposure to UV light (365 nm), featuring yellow (sample A) and red (sample B) colours. The picture in Fig. 6 shows the coloration of the sample prepared with yellow and red dyes, before and after irradiation with UV light.

The samples show a broad band centered between 440 and 500 nm for dye A (yellow) and between 490 and 520 nm for dye B (red). An example of the absorption spectra of the yellow and red dyes embedded in iBu-modified matrix before and after irradiation are shown in Fig. 7.

The most remarkable properties of these materials, such as the absorption spectra upon irradiation with UV light and the kinetic of the bleaching process (recovery of the original whiteness) have been measured in different organically functionalized matrices as a function of the composition of the ormosil matrix and the sol-gel processing parameters.

The stability of the naphthopyran molecules embedded in ormosil matrices is one of the important parameters to take into consideration in optical applications. The UV radiation, needed to operate the photochromic device, is also responsible for the degradation of the photochromic molecules and the progressive loss of the effect.

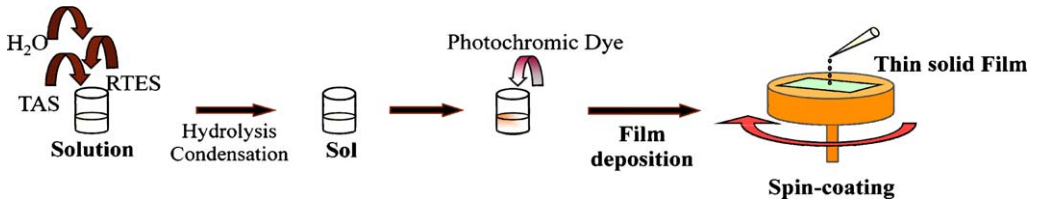

Fig. 4. Scheme of the preparation process of the coatings.

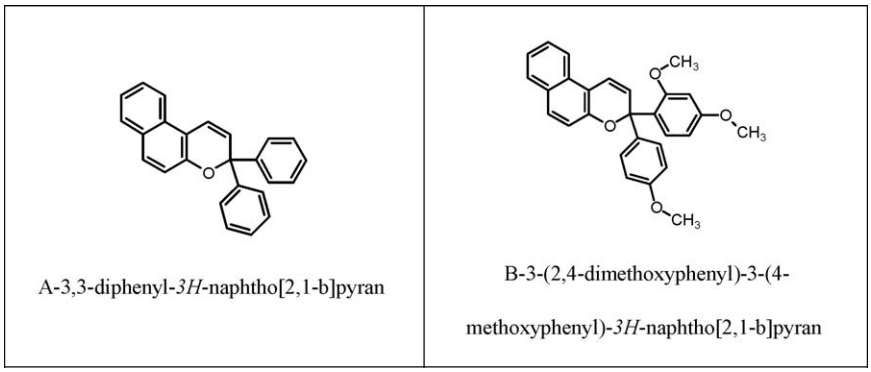

Fig. 5. Chemical structure of the naphthopyran dyes used for samples preparation.

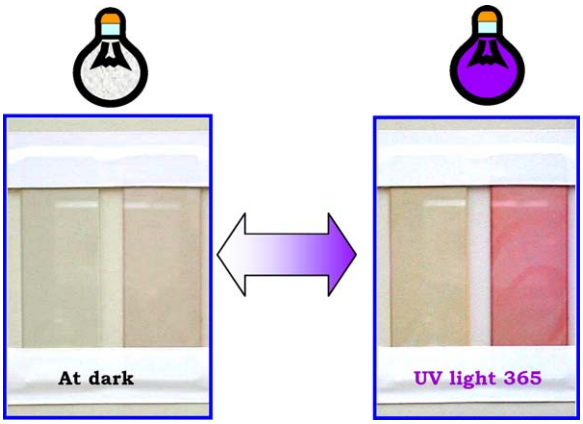

Fig. 6. Photograph of the films prepared with dyes A and B, before and after of the UV irradiation.

4. The role of the organic functional groups in the ormosil matrix on the photochromism of naphthopyrans

Photochromic 3,3-diphenyl-3H-naphtho[2,1-b]pyran molecules (A) were embedded in sol-gel prepared organically modified thin films. The introduction of organic functional groups (Me, Ph or iBu) into a silica matrix allows tailoring the pore surface and the polarity of the environment of the embedded host molecules. The photochromic properties of the naphthopyran molecules depend strongly on the polarity of the pores where the molecules are located and, hence, on these organic groups in the ormosil matrix. The chemical structure of the colourless and coloured forms of the yellow dye [3,4] is given in Fig. 8.

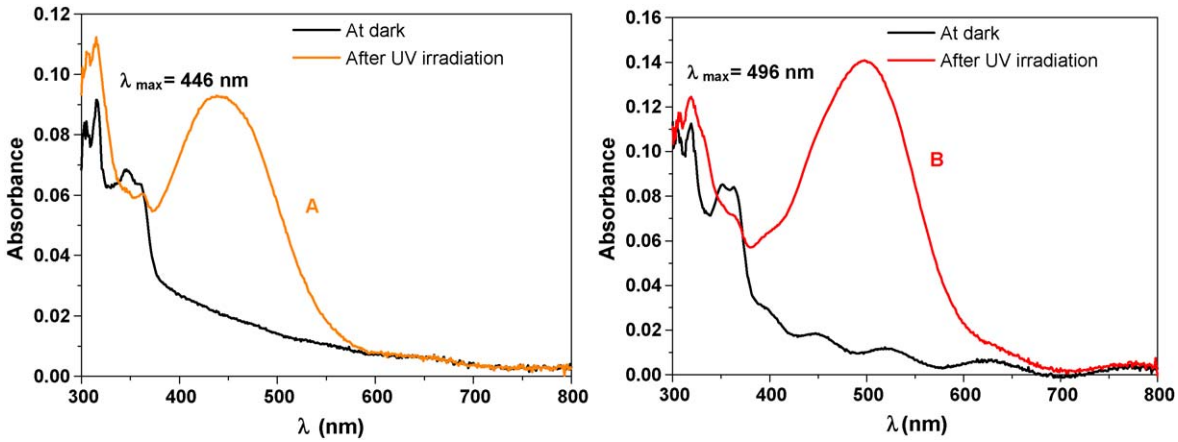

Fig. 7. Absorption spectra of the dye A and B embedded in iBu modified matrix before and after of the irradiation with UV light.

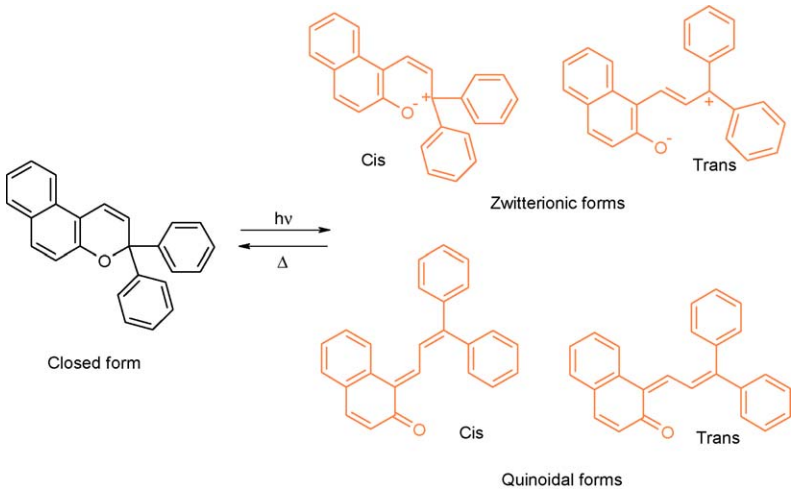

Fig. 8. Chemical structure of the naphthopyran dye (A) used for samples preparation and the possible open coloured forms.

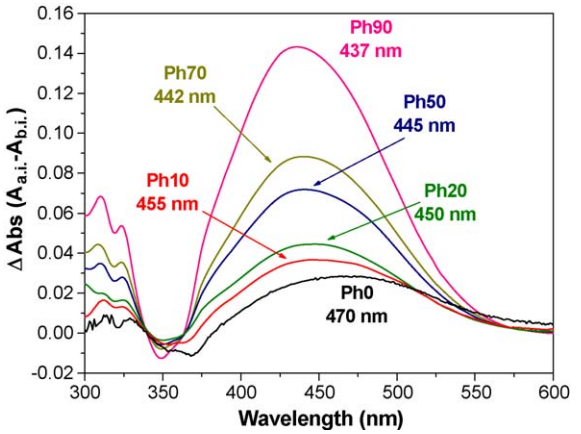

Fig. 9. UV–vis absorption spectra of samples prepared with different amount of Ph groups in the matrix.

Table 2
Spectral position of the absorption band of the yellow naphthopyran in ormosil matrices.

Sample	Me λ_{max} (nm)	Bu λ_{max} (nm)	Ph λ_{max} (nm)
R90	–[a]	439	437
R70	449	440	442
R50	457	444	445
R30	462	446	449
R20	466	446	450
R10	468	459	455
R8	467	463	459
R6	468	467	460
R4	470	468	462
R2	467	463	463
R0	470	470	470

R represents Me, Bu or Ph.
[a] Not possible to measure

4.1. Spectral behavior of yellow naphthopyran embedded in ormosil coatings

The absorption spectra of the resulting films were measured between 300 and 800 nm. All samples showed an absorption band in the 350–365 nm range. Upon irradiation with UV light, the samples acquire a deep coloration showing a broad band centered around 450 nm. The position of the band was found to depend on the matrix used for film preparation. A progressive shift to the UV is observed as the *R*/Si ratio in the matrix is increased. This effect is shown in Fig. 9 for samples prepared in Ph-modified matrices.The position of the band was also found to depend on the nature of the organic substituents used in the matrix. In this sense, samples prepared with iBu and Ph groups showed higher important shifts to the UV as compared with those shown in samples prepared with Me-modified matrices with the same relative amount (Fig. 10).

The position of the absorption band of the different samples prepared in this work is summarized in Table 2 and given as a function of the percentage of Si atoms modified with *R* groups in the matrix in Fig. 11.

The nature and amount of the organic groups (*R*) in the ormosil determine the polarity of the inner surface of the pores, where the photochromic molecules will be located, and therefore their spectral and kinetic properties. In samples prepared without organic substituents (*R*/Si = 0), the surface of the pores in the resulting matrix consists mainly of uncondensed OH groups, which confer a very polar environment to the pore [57.9 kcal/mol in the Reichardt $E_T(30)$ scale] [49]. The incorporation of *R* groups into the structure results in a decrease of the polarity of the matrix as a function

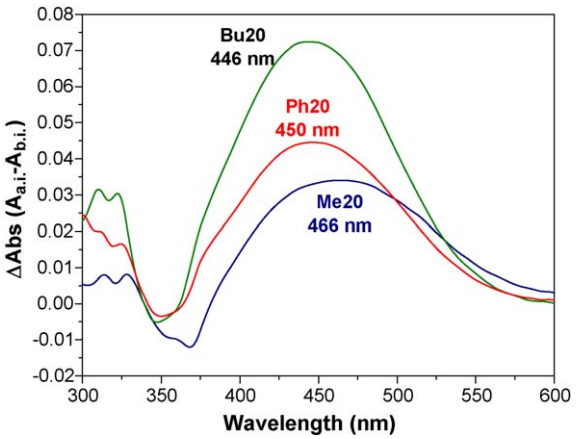

Fig. 10. UV–vis spectra of photochromic naphthopyran molecules (dye A) embedded in ormosils with different modifying groups.

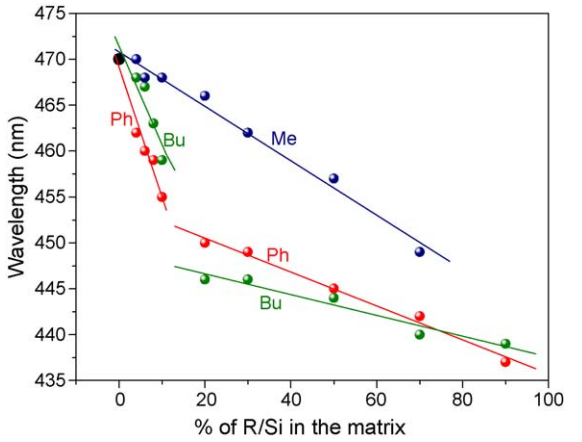

Fig. 11. Position of the absorption band of coloured photochromic films as a function of the *R* groups/Si ratio in the matrix.

of the *R* loading [49,50]. This effect is due to the lower polarity of the *R* groups attached to its surface and the fact that large organic chains may hinder the influence of the OH groups of the pores surface, reducing furthermore the polarity of the cage as sensed by the dye molecule [41]. The representative spectra given in Fig. 9 and the data in Fig. 11 show a progressive blue shift in the absorption maxima as the polarity of the matrix is reduced (the amount of *R* is increased). The difference in polarity of the different organic groups can be observed in the spectra of samples prepared with the same amount of *R* (Fig. 10). An interesting behavior was observed regarding this shift: Samples prepared with Me groups showed a rather linear behavior. Samples prepared with Ph or iBu groups showed two different linear behaviors for low and high *R* contents in the matrix. At very low concentrations of *R* (0–10%), the pore surface is mainly composed of OH groups with a low amount of *R* groups, which have a strong influence over the polarity of the pore. Increasing the amount of *R* groups above 10%, results in a screening of the small OH groups at the surface of the pore. Once this screening is effective, the changes in the *R*/OH ratio in the pore surface have a much lower effect on the polarity. In samples prepared with Me groups, this effect is not observed due to the smaller size of the group, which is not able to effectively screen the OH groups [41].

4.2. Dynamic behavior of the photochromic dye embedded in ormosil coatings

Upon cessation of the UV irradiation, the photochromic films undergo a thermal bleaching (at dark), recovering their original whiteness. Bleaching kinetics were measured by monitoring the light absorption at the peak maxima of the coloured films of the different samples. The kinetic of this bleaching process was also found to follow a bi-exponential decay in most cases and was strongly dependent on the matrix used for the encapsulation of the photochromic molecules. In this sense, increasing the amount of *R* groups in the matrix resulted in a faster bleaching of the samples. In samples prepared with very low *R* loadings ($R \leq 4\%$), the curves followed a first order exponential decay. Fig. 12 shows the kinetics of the thermal bleaching of the photochromic effect in Ph-modified matrices.

The nature of the organic substituents in the matrix also plays an important role in the kinetics of the thermal bleaching. iBu-modified matrices showed faster kinetics as compared with Me- or Ph-modified matrices with the same amount of *R*. The bleaching kinetics of samples

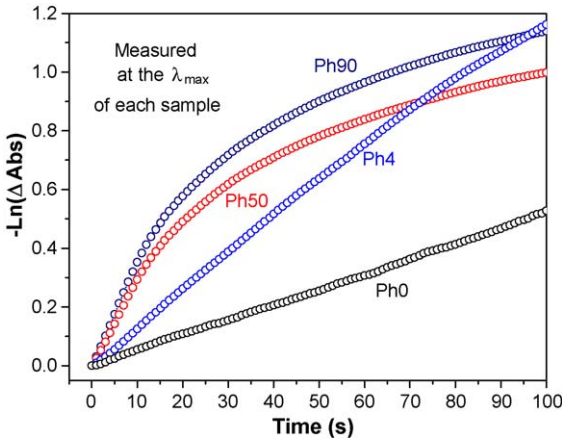

Fig. 12. Thermal bleaching kinetics of the photochromic molecules in Ph-modified matrices.

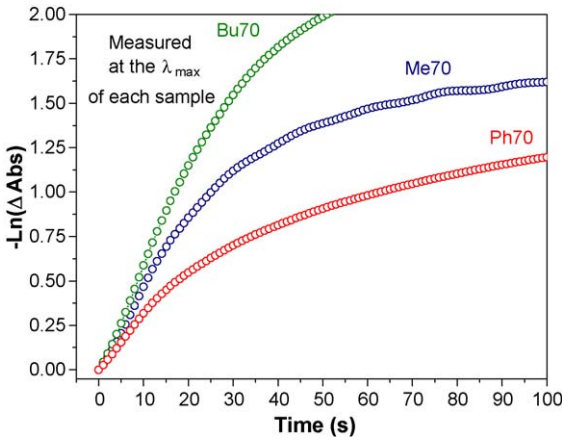

Fig. 13. Thermal bleaching kinetics of the photochromic effect in R70 samples.

Bu70, Me70 and Ph70 are given in Fig. 13 to illustrate this observation. As mentioned before, the kinetics of the thermal bleaching follows a bi-exponential decay. The kinetic data of representative samples measured is

Table 3
Kinetic data of the thermal bleaching of some of the photochromic samples prepared in this work.

Sample	Me			Bu			Ph		
	k_1[a]	k_2[a]	t(s)	k_1[a]	k_2[a]	t(s)	k_1[a]	k_2[a]	t(s)
R90	98.6	8.1	11.8	165.3	–	5.1	84.8	8.6	19.1
R70	81.5	9.6	12.6	122.1	52.3	9.2	69.8	8.4	22.5
R50	74.0	7.2	15.9	102.7	32.8	11.1	73.3	7.6	26.1
R10	84.5	6.1	10.6	42.7	7.0	19.2	44.5	8.0	22.6
R4	47.0	–	17.9	65.4	5.9	13.0	16.6	–	47.6
R0	7.8	–	116	7.8	–	116	7.8	–	116

[a] k values given as $k \times 10^3$ s^{-1}.

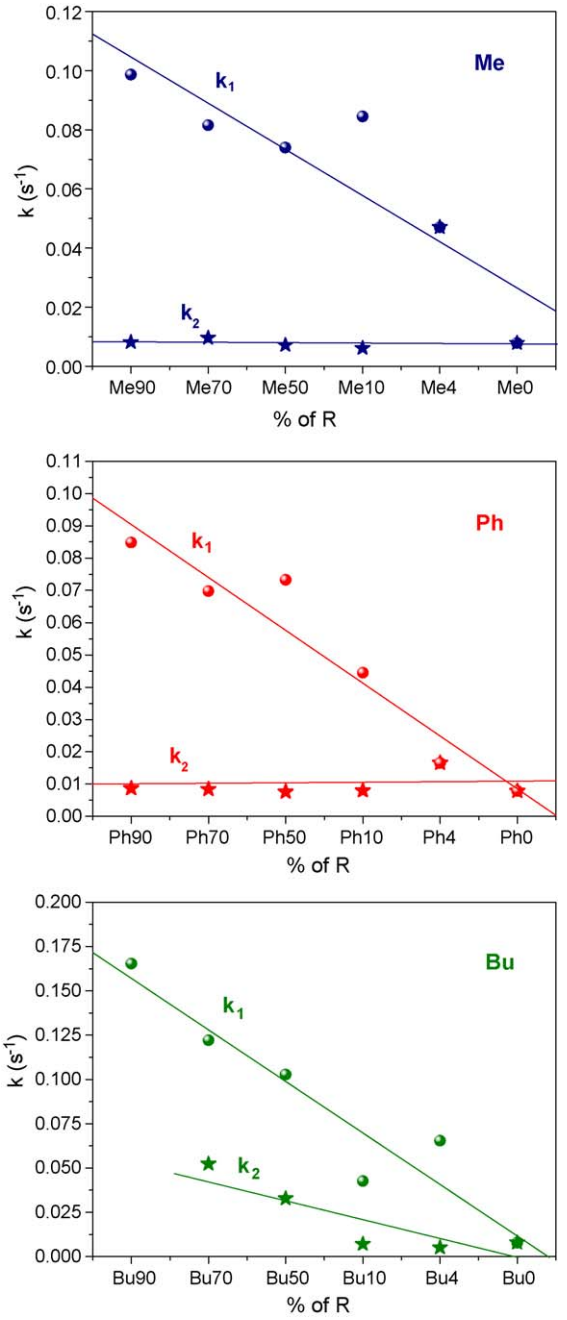

Fig. 14. Kinetic constants of the photochromic naphthopyran molecules in different ormosil matrices (yellow dye).

summarized in Table 3. The kinetic constants k_1 and k_2 of the different samples are represented in Fig. 14.

The kinetic measurements revealed the existence of two decay processes in the matrices having *R* loadings above 4%. The faster kinetic constant of all samples (k_1) was found to increase with the amount of *R* groups in the matrix, while the slower (k_2) remained nearly constant and very close to the value obtained in unmodified matrices (R0) (Fig. 14). This can be explained by the co-existence of two different sites in the matrix allocating photochromic molecules [41]. The first site, rich in OH groups exists in all samples (including those with R90) and gives rise to the slower kinetic constant. The second site, rich in *R* groups and responsible for the fast kinetic constant, was found to increase with the amount of *R* in the sample. An exemption was found for iBu-modified matrices: in contradiction with samples Me90 and Ph90, sample Bu90 shows a single exponential decay kinetic (Fig. 14 and Table 3). Moreover, samples Bu70 and Bu50 show higher k_2-values than the corresponding Me or Ph samples (Fig. 14).

The shape and the larger size of the iBu groups are probably responsible for the more effective screening observed, even in pores with relatively high amounts of OH groups. This observation can also be explained by the formation of micelle like structures in matrices with high iBu loadings [51], able to accommodate the organic dye. In this case, the photochromic molecules will be trapped in an environment with a much lower polarity. The increased flexibility of the iBu groups as compared with Me and Ph groups can also facilitate the movement of the photochromic molecules inside the pore resulting in a faster isomerization kinetics [41].

Another possible explanation for the fast and slow bleaching kinetics found in these samples is the stronger stabilization of the zwitterionic open coloured forms (Fig. 8) of the photochromic dye as compared to the other coloured forms of the dye in environments with higher polarity [2].

5. The influence of sol-gel processing parameters on the photochromic properties of a naphthopyran dye in an ormosil matrix

The photochromic properties of the 3-(2,4-dimethoxyphenyl)-3-(4-methoxyphenyl)-3H-naphtho[2,1-b]pyran (red dye) dispersed in a phenyl-modified ormosil matrix were modified by controlling different parameters of the sol-gel processing, namely the time and temperature of the hydrolysis and condensation of the initial sol, the relative amount of the dye incorporated in the matrix and the curing time of the samples after deposition. Fig. 15 shows the structure of the red naphthopyran dye and some of the different isomers of the open form (merocyanines) embedded in the ormosil matrix. The composition of the ormosil host matrix, however, remained the same for all samples, limiting the effect of the changes to the structure of the matrix.

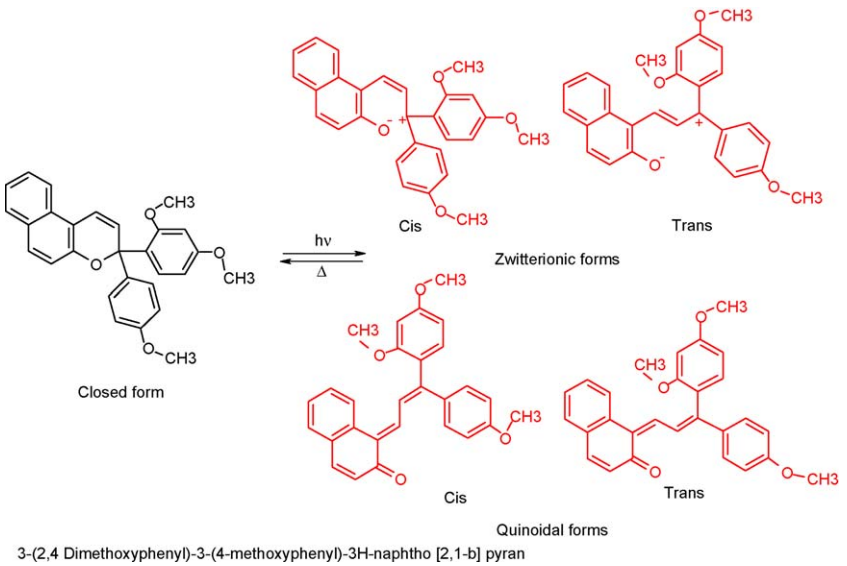

Fig. 15. Chemical structure of the red naphthopyran dye and some of the different isomers of the open form (merocyanines).

5.1. Hydrolysis and condensation: time (t_{hyd}) and temperature (T_{hyd}) of the hydrolysis of the initial sol

The hydrolysis and condensation processes start with the addition of water to the alkoxide precursors. During these processes, the formation and progressive growing of primary silica/ormosil particles takes place. The formation of these particles is strongly influenced by the rates of hydrolysis and condensation, which in turn depend on the temperature of the reaction. Once the sol acquires a certain degree of hydrolysis, it can be deposited on glass substrates. The condensation will then be strongly accelerated due to the massive evaporation of the solvents, forming a solid thin film.

In order to study the effect of the hydrolysis and condensation on the photochromic properties of the coatings, samples were prepared allowing the sol to hydrolyze for different periods of time, keeping constant all other preparation parameters including temperature, which was kept at 25 °C. The results are summarized in Table 4. The minimum hydrolysis time required to obtain transparent samples is about 4 h. Shorter hydrolysis times results in the precipitation of the dye as soon as it is added to the sol. At the early stages of the condensation process, the high amount of uncondensed OH groups is responsible for the highly polar environment in the sol, resulting in a very low solubility of the dye. The polarity of the sol is progressively reduced as the condensation of the OH-groups proceeds, allowing the incorporation of the dye into the sol and the deposition of transparent films.

The absorption spectra (position and intensity of the absorption band) of the photochromic films after irradiation with UV light were not affected by the time of hydrolysis, implying that the pore environment remained unaffected. The thickness of the films, however, was slightly increased in samples prepared

Table 4
Spectroscopic properties of the samples prepared with different hydrolysis times at 25 °C.

t_{hyd} (h)	λ_{max} (nm)	ΔAbs ($A_{a.i.}-A_{b.i.}$)	Thickness, e (μm)	Clear film	Kinetic constants		
					$k_1/10^{-3}$ (s^{-1})	$k_2/10^{-3}$ (s^{-1})	t (s)
2.00	–	–	–	x	–	–	–
4.00	488	0.098	–	√x	–	–	–
7.00	487	0.103	1.30	√	12.6	0.64	522.0
15.00	488	0.108	1.35	√	17.1	0.68	492.0
24.00	490	0.109	1.38	√	22.2	0.86	316.4

All samples have a dye:Si ratio of 0.005:1 and curing time of 24 h.

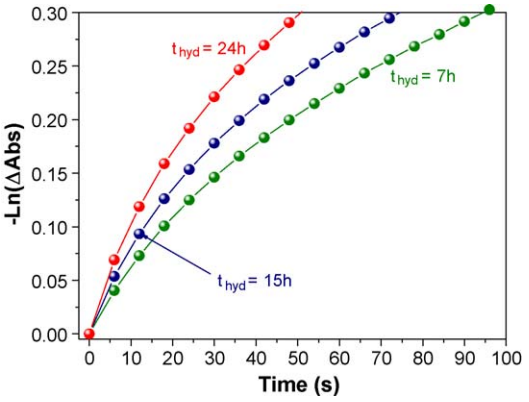

Fig. 16. Thermal bleaching kinetics of photochromic samples with different hydrolysis times at 25 °C.

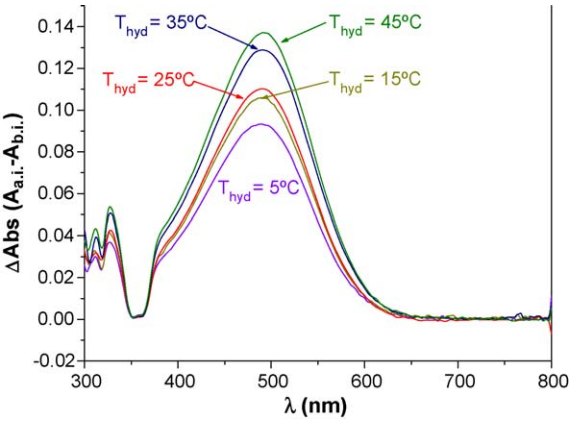

Fig. 17. Absorption spectra of the samples prepared with different temperatures of hydrolysis.

with longer hydrolysis times due to the increased viscosity of the sols.

An interesting behaviour was observed in the bleaching kinetics of samples prepared with different t_{hyd}. The samples exhibited higher fading rates in the dark (faster thermal bleaching) as the hydrolysis time was increased. The measured bleaching curves, represented as –Ln(ΔAbs) versus time, are shown in Fig. 16. The kinetic data of the representative samples measured are summarized in Table 4. The slower bleaching kinetics observed in samples with t_{hyd} = 7 h is related to a lower relative amount of Ph groups in the pore surface. The presence of Ph groups in the matrix-dye interface boosts the bleaching kinetics of the naphthopyran dyes in sol-gel prepared ormosil matrices [41]. The hydrolysis and condensation rates of alkoxides are much higher than those of organically modified alkoxides: in mixtures of silicon alkoxides and silicon alkoxides modified with organic groups (*R*), the sol can be considered as growing silica clusters having the *R*-modified silicon alkoxides as a co-solvent [52], increasing their size as the hydrolysis proceeds. Immediately after the deposition of the film, the rapid release of solvents leads to the condensation of the phenyl-modified alkoxides at the surface of the silica primary particles. The larger the silica primary particles at the time of deposition, the larger the relative amount of Ph groups on the surface of the resulting pores.

The temperature of the hydrolysis (T_{hyd}) has also an important effect on the photochromic properties of the resulting thin films. Samples were allowed to hydrolyze for 24 h at different temperatures between 5 and 45 °C, keeping constant all other parameters. The absorption spectra of samples prepared with different T_{hyd}, after irradiation with UV light, are shown in Fig. 17.

The position of the absorption maxima of the samples remained constant at ≈ 490 nm despite the T_{hyd} used for their preparation. However, an increase of the intensity of the band and the thickness of the films was observed as the T_{hyd} was increased, as shown in Table 5. Both, the hydrolysis and condensation processes in the sol are accelerated by temperature. For a given t_{hyd}, higher T_{hyd} leads to the formation of larger silica primary particles in the sol, resulting in an increase of the viscosity and therefore a thicker spin-coated film. The intensity of the absorption maximum as well as the thickness of the films, depicted as a function of the T_{hyd}, are shown in Fig. 18a. The absorption intensity, however, after being normalized with the thickness according to Beer Lambert's law, decreased considerably with the increase of the T_{hyd}, as shown in Fig. 18b. At higher T_{hyd}, the polarity of the pore environment is reduced due to the higher relative amount of Ph groups (vs. OH groups) that interact with naphthopyran molecules inside the pore cage [41]. The latter results in higher stabilization of the closed form of the photochromic molecule reducing, therefore, the colour intensity of the sample after irradiation.

The T_{hyd}, although affecting strongly the spectral behaviour of the photochromic samples, has no influence on the bleaching kinetic, having all samples k_1 and k_2 kinetic constants of about 0.019 s^{-1} and 7.9×10^{-4} s^{-1} respectively. We should expect a similar behaviour to that observed for different t_{hyd} at 25 °C, where the bleaching was considerably accelerated increasing the hydrolysis time from 0 to 24 h. This effect, however, can only be observed at the first stages of the hydrolysis when a rapid growing of the silica particles occurs. After 24 h of hydrolysis, the size of the primary silica particles in the sol stabilizes, and even

Table 5
Spectroscopic properties of the samples prepared with different temperatures of hydrolysis.

T_{hyd} (°C)	λ_{max} (nm)	ΔAbs ($A_{a.i.}-A_{b.i.}$)	Thickness, e (μm)	ΔAbs/e (nm^{-1})
5	490	0.093	0.90	0.103
15	490	0.106	1.23	0.088
25	490	0.109	1.38	0.079
35	492	0.128	1.87	0.068
45	492	0.137	2.10	0.065

All samples were hydrolyzed for 24 h, using a dye:Si ratio of 0.005:1 and cured at 100 °C for 24 h.

though condensation of the sol continues to take place, it has very limited effect on the relative amount of phenyl groups on the pore surface of the resulting film, and hence on the interaction between the dye and the pore surface.

5.2. Amount of photochromic dye in the matrix

The amount of photochromic dye that is incorporated in the ormosil matrix is a key issue to determine the intensity of the absorption of the resulting coating. At the same time, the addition of very large amounts of naphthopyran to the composition will lead to the precipitation of the dye in the pores hindering the photochemical ring opening process. Therefore, it is important to optimize the concentration of dye as a function of the overall performance of the photochromic coatings. In the samples described here, a linear increase of the ΔAbs ($A_{a.i.}-A_{b.i.}$) of the irradiated samples was observed as the dye/Si ratio was increased, reaching a saturation value around dye/Si = 0.02 as shown in Table 6.

Table 6
Spectroscopic properties of the samples prepared with different red dye/Si ratios.

Dye/Si molar ratio	λ_{max} (nm)	ΔAbs ($A_{a.i.}-A_{b.i.}$)	Thickness, e (μm)	ΔAbs/e (μm^{-1})
0.0025	490	0.046	1.40	0.033
0.0050	490	0.109	1.38	0.079
0.0075	490	0.113	1.23	0.092
0.0100	489	0.154	1.20	0.128
0.0125	488	0.170	1.15	0.148
0.0150	488	0.174	1.10	0.158
0.0175	490	0.202	0.93	0.217
0.0200	490	0.212	0.91	0.233
0.0225	490	0.180	0.91	0.198
0.0250	492	0.209	0.89	0.235
0.0275	492	0.209	0.88	0.237
0.0300	490	0.213	0.85	0.251

The absorption spectra of irradiated samples prepared with different amounts of dye are shown in Fig. 19. The position of the absorption band, being around 490 nm, is not affected by the amount of dye in the matrix. The thickness of the coating decreased as higher dye/Si ratios were used. This issue, shown in Fig. 20a, is due to the dilution of the sol by the addition of the dye solution (in THF). The ΔAbs at the maximum absorption of the samples normalized with their thickness is given in Fig. 20b. The kinetics of the thermal bleaching was not affected by the amount of dye embedded in the matrix.

5.3. Curing of the samples after film deposition

The samples after deposition must undergo a heat treatment in order to consolidate the structure of the embedding matrix and allow the formation of a

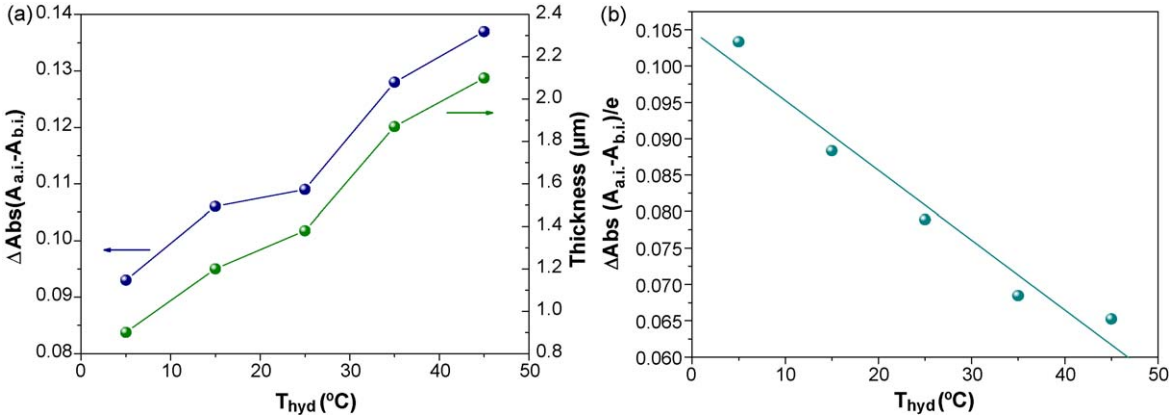

Fig. 18. (a) Influence of the temperature of the hydrolysis on the ΔAbs ($A_{a.i.}-A_{b.i.}$) and the thickness of the resulting samples. (b) The intensity of the absorption maximum of the irradiated samples normalized with the thickness.

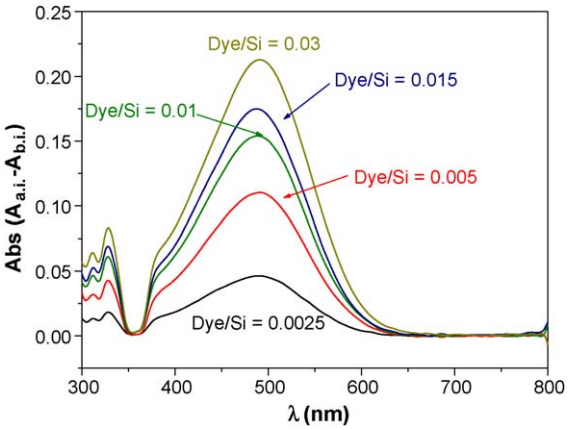

Fig. 19. Absorption spectra of the samples prepared with different amount of red dye.

mechanically stable coating. At room temperature, this process is very slow and could take months to achieve a stable coating. On the other hand, at high temperatures, the organic dye may decompose, losing its photochromic properties. The curing temperature was therefore set to 100 °C, achieving stable layers in a reasonable period of time and avoiding the decomposition of the dye in the matrix. The time of curing was found to have an important effect on the properties of the photochromic coatings. Samples prepared with 24 h of hydrolysis at 25 °C and a dye:Si ratio of 0.005:1 were deposited and cured for different periods of time, ranging from 0 to 166 h. The photochromic properties of these samples are summarized in Table 7.

The absorption spectra of the samples, after irradiation with UV-light, are given in Fig. 21. The absorption maxima of the samples (λ_{max}) showed a progressive shift to lower wavelengths along with the time of curing, reaching a constant value after approximately 24 h as shown in Fig. 22. At the same time, a decrease in both the ΔAbs ($A_{a.i.}-A_{b.i.}$) at the band maxima and the thickness of films was observed in the first 24 h of curing, as shown in Table 7, reaching then a constant value. The ΔAbs as a function of the curing time is given in Fig. 22, after normalization with the thickness.

Table 7
Spectroscopic properties of the samples with different curing time at 100 °C.

Curing time (h)	λ_{max} (nm)	ΔAbs ($A_{a.i.}-A_{b.i.}$)	Thickness, e (μm)	ΔAbs/e (nm^{-1})
0	498	0.124	1.57	0.078
5	492	0.125	1.44	0.087
15	490	0.111	1.39	0.080
24	488	0.109	1.38	0.079
48	488	0.103	1.38	0.075
72	488	0.111	1.38	0.081
96	488	0.099	1.38	0.072
120	488	0.092	1.38	0.067
144	488	0.107	1.38	0.078
166	488	0.090	1.38	0.065

The relatively slow thermal bleaching kinetics observed for as-deposited dry samples was progressively accelerated (decrease of $t_{1/2}$) with the curing of the samples, as shown in Fig. 23. The kinetic data of the representative samples measured are summarized in Table 8. All this observations can be explained by the progressive condensation of the glass matrix during the curing process, releasing water and solvents and leading to a closer pore structure, increasing, hence, the chemical and steric interactions between the photochromic molecules and the matrix pore surface [40]. Differently to the effect of the hydrolysis time on the

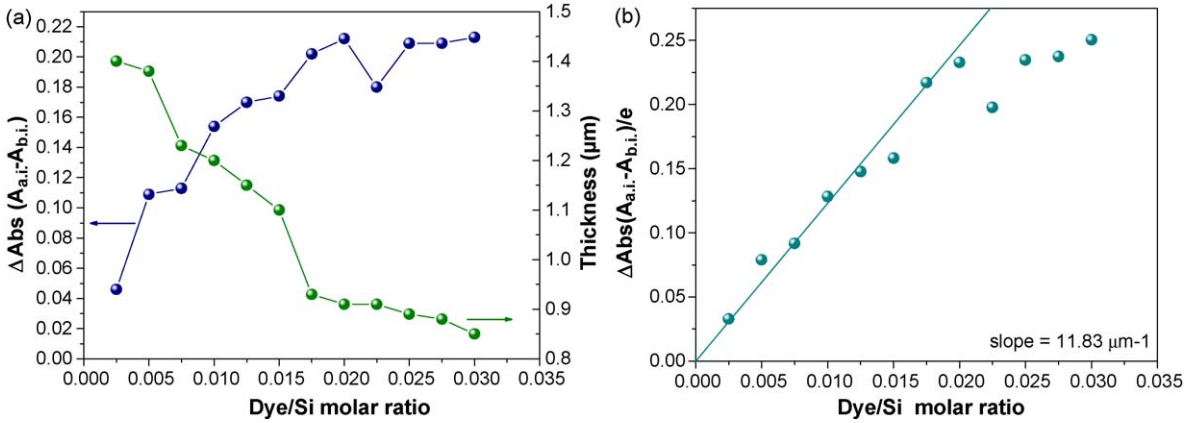

Fig. 20. (a) Effect of the amount of red dye in the spectroscopic properties of the samples. (b) The ΔAbs ($A_{a.i.}-A_{b.i.}$) normalized with the thickness of the samples.

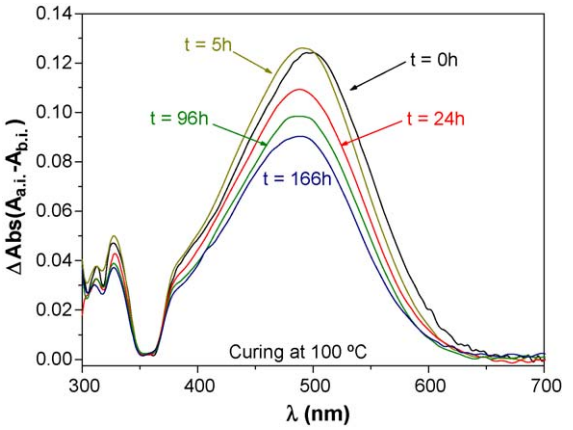

Fig. 21. Absorption spectra of the samples with different curing time.

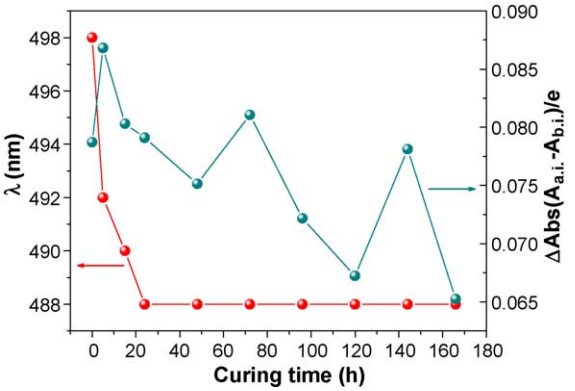

Fig. 22. Effect of curing time on the resulting samples.

bleaching kinetics, which is due to the concentration of phenyl groups on the pore surface, the curing time affects the steric interactions between the dye and the pore surface due to the contraction of the pore walls during the curing process [42].

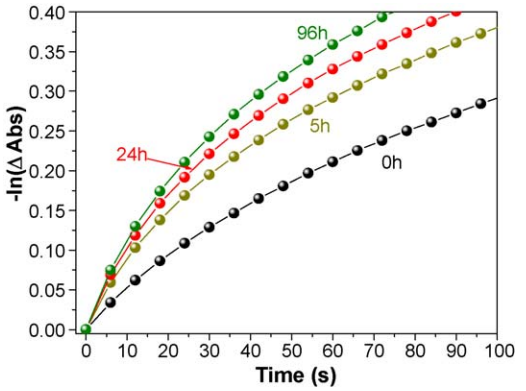

Fig. 23. Thermal bleaching kinetics of the photochromic effect in samples with different curing time at 100 °C.

Table 8
Kinetic data for the thermal bleaching of some of the photochromic samples with different curing time.

Curing time (h)	Kinetic constants		
	$k_1/10^{-3}$ (s^{-1})	$k_2/10^{-3}$ (s^{-1})	t (s)
0	9.6	0.58	496.6
5	17.2	0.75	378.5
24	22.2	0.86	316.4
96	26.6	1.02	265.2

6. Photostability of a photochromic naphthopyran dye in different sol-gel prepared ormosil coatings

The photodegradation of the 3-(2,4-dimethoxyphenyl)-3-(4-methoxyphenyl)-3H-naphtho[2,1-b]pyran (red dye) upon prolonged exposition to UV light was measured in different ormosil matrices. The absorbance of the photochromic film was monitored versus time while irradiating with a UV lamp, to follow the photodegradation of the photochromic molecules. It was found that the photodegradation of the naphthopyran dye is strongly affected by the composition of the embedding ormosil matrix. The introduction of organic substituents into matrices results in an important reduction of the relative amount of silanol groups in the inner pore surface, where the molecules are located. This, in turn, has an important effect on the polarity of the matrix and, therefore, on the photostability of the dye molecules. The photodegradation of the naphthopyran molecules in the sol-gel matrices prepared here showed no yellowing of the matrix, even when exposed to intense UV-light for 120 h, due to the high photochemical stability of the ormosil matrices.

The photostability of the naphthopyran molecules in ormosil matrices is largely increased as the relative amount of the organic substituent is increased. Fig. 24 shows the degradation curves of the dye in matrices with different loadings of Ph groups. Samples with *R*/Si ratios ≥ 0.3 show no difference in photostability since most of the NP molecules are in pores rich in Ph groups. The much faster photodegradation observed in matrices with *R*/Si ratios lower than 0.3 can be explained by the lower porosity of the matrices that forces the NP molecules to occupy pores rich in OH groups [53,54]. In this polar environment, the zwitterionic forms of the open coloured form of the dye are stabilized, allowing the interaction with the pore surface via hydrogen bonding or ionic interactions [55], favouring the degradation of the photochromic molecules. The degradation of the naphthopyran molecules leads

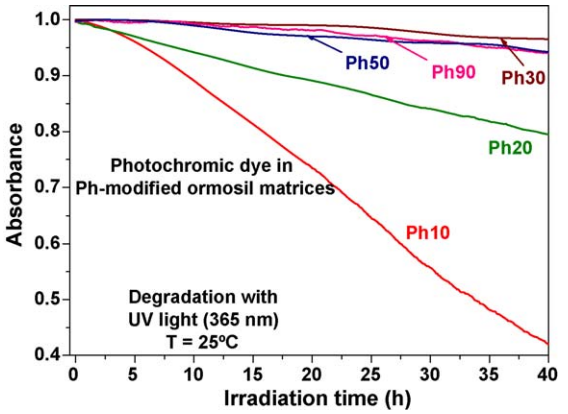

Fig. 24. Photodegradation of red dye embedded in Ph-modified matrices with different amount of Ph groups.

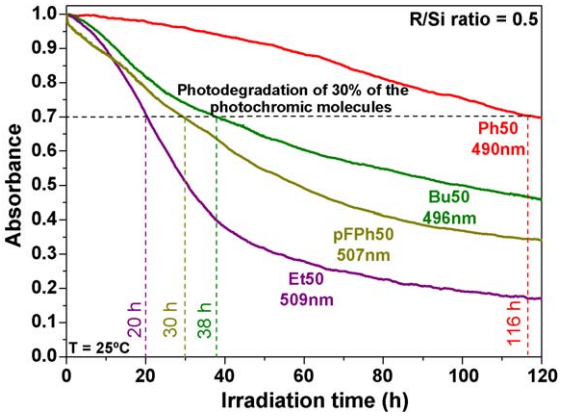

Fig. 25. Photodegradation of red dye embedded in different ormosil matrices.

mainly to the formation of benzophenones, β-phenylcynnamaldehydes and other minor photoproducts [56–60].

An interesting behaviour was observed in the photostability of the photochromic films prepared with the same amount of different organic functional groups. The usage of larger organic functional groups in the ormosil resulted in a substantial increase of the photostability of the NP molecules in these matrices. Fig. 25 shows the photodegradation of the photochromic dye in ormosil matrices prepared with different organic groups. In this way, the photodegradation of the photochromic molecules in Ph-modified samples is reduced by a factor of 5, as compared with the photodegradation of the molecules in Et-modified matrices. The degradation of 30% of the photochromic molecules in Ph-modified matrices requires 116 h of irradiation, whereas it takes only 20 h in Et-modified matrices (Fig. 25). The decrease of the polarity of the pore environment, as larger modifying groups are used in the ormosil, results in an increase of the photostability of the naphthopyran molecules.

7. Conclusions

The properties of different photochromic naphthopyran molecules embedded in thin-film ormosil matrices prepared by the sol-gel method can be controlled by the composition of the host matrix. The ormosil matrix allows the incorporation of an important amount of photochromic molecules in thin glass films as required in most applications of photochromic coatings. The nature and amount of the organic functional groups ($-CH_3$, $-C_2H_5$, $-C_3H_7$, $-C_4H_9$, $-C_6H_5$ and $-C_6F_5$) incorporated in the network of the ormosil matrices, as well as the parameters of the sol-gel processing, affect the size and shape of the pores and the chemical composition of their surface, and determine the polarity of the inner surface of the pores, where the photochromic molecules will be located. Therefore, it provides a way of controlling the photochromic properties of the naphthopyran in ormosil coatings and hence, their absorption spectra and the bleaching kinetics, which are greatly affected by the polarity of the environment.

The photostability of the photochromic molecules embedded in ormosil matrix upon prolonged exposition to UV light was found to depend strongly on the nature of the embedding matrix. The introduction of organic functional groups into the inner pore surface of the matrix affects the stability of the molecules, in terms of the effectiveness of the interaction between the photochromic molecules and the surface of the pores, and can be used as an important tool to increase the photostability of the photochromic dye in a device.

The ability to control the photochromic properties and the photostability of the naphthopyran molecules by varying the chemical composition of the embedding matrix and the sol-gel preparation and processing parameters is of great interest for the design of materials with defined properties.

Acknowledgments

This work was supported by a research project from MICINN (MAT2008-00010/NAN). Rosario Pardo is grateful to MEC for a research contract ‘‘Juan de la Cierva’’.

References

[1] R.S. Becker, J. Michl, J. Am. Chem. Soc. 88 (1966) 5931.
[2] B. Van Gemert, J.C. Crano, R. Guglielmetti (Eds.), Organic Photochromic and Thermochromic Compounds, 1, Plenum Press, New York, 1999, Ch 3.
[3] B. Van Gemert, A. Kumar, D.B. Knowles, Mol. Cryst. Liq. Cryst. 297 (1997) 131.
[4] A. Kumar, Mol. Cryst. Liq. Cryst. 297 (1997) 139.
[5] C. Lenoble, R.S. Becker, J. Photochem. 33 (1986) 187.
[6] B.Van Gemert, M.P. Bergoni, US Patent 5,066,818 (1991).
[7] D.B. Knowles, US Patent, 5,238,981 (1993).
[8] B. M. Heron, C. D. Gabbutt, J. D. Hepworth, S. M. Partington, D. A. Clarke, S. N. Corns, WO20010112619 (2001).
[9] B. Oliver, B. Rodrigue, C. Y. Ping, J. Patrick, FR2837200 (2003).
[10] X. Blin, J-C. Simon, FR2845910 (2004).
[11] X. Blin, J-C. Simon JP2004137280 (2004).
[12] M. Viková, Color and Paints, Interim Meeting of the International Color Association, in : Proceedings, 2004.
[13] J.J. Luthern, Mol. Cryst. Liq. Cryst. 297 (1997) 155.
[14] H.G. Heller, J.R. Levell, D.E. Hibbs, D.S. Hughes, M.B. Hursthouse, Mol. Cryst. Liq. Cryst. 297 (1997) 123.
[15] M. Frigoli, C. Moustrou, A. Samat, R. Guglielmetti, Helv. Chim. Acta 83 (2000) 3043.
[16] J.L. Pozzo, G. Harié, V. Lokshin, A. Samat, R. Guglielmetti, Mol. Cryst. Liq. Cryst. 297 (1997) 255.
[17] B.Van Gemert, A. Kumar, US Patent 5,466,398 (1995).
[18] C.D. Gabbutt, T. Gelbrich, J.D. Hepworth, B.M. Heron, M.B. Hursthouse, S.M. Partington, Dyes Pigm. 54 (2002) 79.
[19] C.I. Martins, P.J. Coelho, L.M. Carvalho, A.M.F. Oliveira-Campos, Tetrahedron Lett. 43 (2002) 2203.
[20] D.B. Knowles, B.Van Gemert, US Patent 5,674,432 (1997), (and references therein).
[21] C.M. Nelson, A. Chopra, D.B. Knowles, B.Van Gemert, A. Kumar, US Patent 6,348,604 (2002) (and references therein).
[22] B. Luccioni-Houzé, M. Campredon, R. Guglielmetti, G. Giusti, Mol. Cryst. Liq. Cryst. 297 (1997) 161.
[23] F. Ortica, A. Romani, F. Blackburn, G. Favaro, Photochem. Photobiol. Sci. 1 (2002) 803.
[24] H. Görner, A.K. Chibisov, J. Photochem. Photobiol. A 149 (2002) 83.
[25] A. Kumar, B.Van Gemert, D.B. Knowles, US Patent 5,458,814 (1995).
[26] A. Rivaton, J.-L. Gardette, B. Mailhot, S. Morlat-Therlas, Macromol. Symp. 225 (2005) 129.
[27] S. Nespurek, J. Pospisil, J. Optoelectron. Adv. M 7 (2005) 1157.
[28] C.J. Brinker, G.W. Sherer, Sol-Gel Science: The Physics and Chemistry of Sol-Gel Processing, Academic Press, San Diego, 1990.
[29] D. Avnir, D. Levy, R. Reisfel, J. Phys. Chem. 88 (1984) 5956.
[30] D. Levy, D. Avnir, J. Phys. Chem. 92 (1988) 4734.
[31] D. Levy, L. Esquivias, Adv. Mater. 7 (1995) 120.
[32] D. Levy, Chem. Mater. 9 (1997) 2666.
[33] C. Guermeur, C. Sanchez, B. Schaudel, K. Nakatami, J.A. Delaire, F. de Monte, D. Levy, SPIE Sol-Gel Optics IV 3136 (1997) 10.
[34] D. Levy, S. Einhorn, D. Avnir, J. Non Cryst. Solids 113 (1989) 137.
[35] L. Hou, B. Hoffmann, M. Mennig, H. Schmidt, J. Sol Gel Sci. Technol. 2 (1994) 635.
[36] L. Hou, H. Schmidt, Matt. Lett. 27 (1996) 215.
[37] J. Biteau, G.M. Tsivgoulis, F. Chaput, J.P. Boilot, S. Gilat, S. Kawai, J.M. Lehn, B. Darracq, F. Martin, Y. Levy, Mol. Cryst. Liq. Cryst. 297 (1997) 65.
[38] J. Biteau, F. Chaput, J.P. Boilot, J. Phys. Chem. 100 (1996) 9024.
[39] W.S. Kwak, J.C. Crano, PPG Tech. J. 2 (1996) 45.
[40] M. Zayat, D. Levy, J. Mater. Chem. 13 (2003) 727.
[41] M. Zayat, R. Pardo, D. Levy, J. Mater. Chem. 13 (2003) 2899.
[42] R. Pardo, M. Zayat, D. Levy, J. Mater. Chem. 15 (2005) 703.
[43] R. Pardo, M. Zayat, D. Levy, J. Mater. Chem. 16 (2006) 1734.
[44] D. Levy, F. de Monte, J.M. Otón, G. Fiskman, I. Matías, P. Datta, M. López-Amo, J. Sol Gel Sci. Technol. 8 (1997) 931.
[45] D. Levy, M. López-Amo, J.M. Otón, F. del Monte, P. Datta, I. Matías, J. Appl. Phys. 77 (1995) 2804.
[46] D. Levy, Mol. Cryst. Liq. Cryst. 297 (1997) 31.
[47] O. Levy, S. Shalom, I. Benjamin, G. Perepelitsa, A.J. Agranat, R. Neumann, Y. Avny, D. Davidov, Syn. Met. 102 (1999) 1178.
[48] X.D. Sun, X.J. Wang, W. Shan, J.J. Song, M.G. Fan, E.T. Knobbe, J. Sol Gel Sci. Technol. 9 (1997) 169.
[49] C. Rottman, G. Grader, D. Avnir, Chem. Mater. 13 (2001) 3631.
[50] C. Rottman, G.S. Grader, Y. De Hazan, D. Avnir, Langmuir 12 (1996) 5505.
[51] H. Frenkel-Mullerad, D. Avnir, Chem. Mater. 12 (2000) 3754.
[52] U. Schubert, N. Hüsing, A. Lorenz, Chem. Mater. 7 (1995) 2010.
[53] R. Pardo, M. Zayat, D. Levy, J. Sol Gel. Sci. Technol. 40 (2006) 365.
[54] R. Pardo, M. Zayat, D. Levy, J. Photochem. Photobiol. A Chem. 198 (2008) 232.
[55] B. Dunn, J.I. Zink, Chem. Mater. 9 (1997) 2280.
[56] C. Salemi-Delvaux, M.C. Aubert, G. Campredon, R. Giusti, Guglielmetti, Mol. Cryst. Liq. Cryst. 298 (1997) 45.
[57] C. Salemi-Delvaux, G. Giusti, R. Guglielmetti, Mol. Cryst. Liq. Cryst. 298 (1997) 53.
[58] V. Malatesta, J. Hobley, C. Salemi-Delvaux, Mol. Cryst. Liq. Cryst. 344 (2000) 69.
[59] R. Demadrille, M. Campredon, R. Guglielmetti, G. Giusti, Mol. Cryst. Liq. Cryst. 345 (2000) 1.
[60] G. Baillet, Mol. Cryst. Liq. Cryst. 298 (1997) 75.